

Renormalization group approach to neutron matter: quasiparticle interactions, superfluid gaps and the equation of state

Achim Schwenk^{(a) 1}, Bengt Friman^{(b) 2} and Gerald E. Brown^{(a) 3}

^(a) *Department of Physics and Astronomy, State University of New York,
Stony Brook, N.Y. 11794-3800, U.S.A.*

^(b) *Gesellschaft für Schwerionenforschung, Planckstr. 1, 64291 Darmstadt,
Germany*

Abstract

Renormalization group methods can be applied to the nuclear many-body problem using the approach proposed by Shankar. We start with the two-body low momentum interaction $V_{\text{low } k}$ and use the RG flow from the particle-hole channels to calculate the full scattering amplitude in the vicinity of the Fermi surface. This is a new straightforward approach to the many-body problem which is applicable also to condensed matter systems without long-range interactions, such as liquid ^3He . We derive the one-loop renormalization group equations for the quasiparticle interaction and the scattering amplitude at zero temperature. The RG presents an elegant method to maintain all momentum scales and preserve the antisymmetry of the scattering amplitude. As a first application we solve the RG equations for neutron matter. The resulting quasiparticle interaction includes effects due to the polarization of the medium, the so-called induced interaction of Babu and Brown. We present results for the Fermi liquid parameters, the equation of state of neutron matter and the $^1\text{S}_0$ superfluid pairing gap.

PACS: 21.65.+f; 71.10.Ay; 11.10.Hi

Keywords: Neutron matter; Fermi liquid theory; Renormalization Group; Polarization Effects; Superfluidity

¹ E-mail: aschwenk@nuclear.physics.sunysb.edu

² E-mail: b.friman@gsi.de

³ E-mail: popenoe@nuclear.physics.sunysb.edu

1 Introduction

Fermi liquid theory is a prototype effective theory, invented by Landau in the late 1950's [1,2,3]. In this theory the properties of normal Fermi liquids at zero temperature are encoded in a few parameters, which are related to the effective two-fermion interaction. Over the years, Fermi liquid theory has proven to be an extremely useful tool for studying normal Fermi liquids, in particular liquid ^3He [4]. The main assumption is that the elementary, low-lying excitations of the interacting system are relatively long-lived quasiparticles, with properties resembling those of free particles. The remaining strength in the spectral function is distributed over modes that add up incoherently. In the language of the renormalization group, the incoherent background is integrated out into the quasiparticle interaction, which can be determined by comparison with experiment or by microscopic calculations.

Babu and Brown later realized [5] that, in order to satisfy the Pauli principle in microscopic calculations, one has to take into account not only the particle-hole channel considered by Landau, which gives rise to the propagation of zero sound, but also the exchange channel thereof. This is taken into account in the induced interaction, which incorporates the response of the many-body medium to the presence of the quasiparticles.

Almost a decade ago, Shankar revived the interest in Fermi liquid theory by developing a renormalization group (RG) approach to interacting Fermi systems (for an introduction see Shankar [6] and the lecture notes of Polchinski [7]). Since Fermi liquid theory is restricted to low-lying excitations in the vicinity of the Fermi surface, normal Fermi systems are amenable to the renormalization group, where one has precisely such a separation of modes in mind. Moreover, by taking the loop contributions from both particle-hole channels into account, the RG flow remains antisymmetric, i.e., at any step of the renormalization, the scattering amplitude obeys the Pauli principle and consequently the solution obeys the Pauli principle sum rules. Thus, the antisymmetry of the scattering amplitude, which was the guiding principle of Babu and Brown, is realized naturally in the RG approach. Recently, we obtained additional RG invariant constraints [8]. These approximate constraints are analogous to those obtained by Bedell and Ainsworth for paramagnetic Fermi liquids [9].

In this paper, we solve the one-loop RG equations in the particle-hole channels at zero temperature and in three dimensions. We work in the approximation that both particle-hole momentum transfers are small compared to the Fermi momentum. The justification for this approximation is two-fold: In Fermi liquid theory the long-wavelength excitations play a central role. Hence, our primary aim is to treat these correctly. Furthermore, for the case of nuclear or neutron matter, the dependence of the induced interaction on Landau angle is

fairly weak [10,11]. Thus, we expect an expansion in momentum transfers to be accurate at least for the Fermi liquid parameters.⁴ In this approximation the treatment of the particle-hole phase space with cutoffs is enormously simplified. An RG analysis of a schematic model, including the complete particle-hole phase space in two dimensions, is discussed in [12]. Improved RG equations, beyond one-loop order, are presented in [8].

Here we apply the RG techniques to neutron matter, where the tensor force does not contribute in the S-wave. In this system, a further physical motivation for expanding in small momentum transfers over the Fermi momentum is provided by the unique low momentum nucleon-nucleon interaction $V_{\text{low } k}$ [13,14], which we employ as the starting point for the RG flow. As shown in Figs. 2 and 4 of Bogner *et al.* [14], $V_{\text{low } k}$ is significant only for relative momenta $k < 1.3 \text{ fm}^{-1}$. Moreover, from the evolution of $V_{\text{low } k}$ shown in Fig. 5 of [14] we deduce that the important momentum modes are around the pion mass $m_\pi \approx 0.7 \text{ fm}^{-1}$, since higher momenta do not renormalize $V_{\text{low } k}$ considerably. Therefore, the typical momentum transfer is small compared to the Fermi momentum of neutron matter at nuclear matter density $k_F = 1.7 \text{ fm}^{-1}$.

The main idea of the RG approach to the many-body problem is to “adiabatically” include the in medium corrections to the effective interaction by solving the RG flow equations in the relevant channels. In this exploratory calculation we include the particle-hole channels, which play a special role in Fermi liquid theory. The main effect of scattering in the particle-particle channel, the removal of the short-range repulsion, is taken care of by using $V_{\text{low } k}$ as the starting point for the RG flow. The low-lying excitations in this channel, which are responsible e.g., for superfluidity, are not included. These are then treated explicitly in Section 4.2, where we compute the superfluid gap by employing BCS theory for the particle-hole reducible scattering amplitude.

In the RG approach, the width of the momentum shell that is integrated out in one iteration is a “small parameter”. The full scattering amplitude is an RG invariant quantity. In a conventional approach, this is calculated from a “set of diagrams” while in the RG approach it is continuously evolved from the starting interaction by gradually including the many-body corrections from the narrow momentum shells one at a time. In this sense the RG provides a method for dealing with strongly interacting systems, where perturbation theory fails. We stress that this application of the renormalization group to many-body systems is only indirectly related to the well known RG treatment of critical phenomena.

We derive the one-loop renormalization group equations for the quasiparticle interaction and the scattering amplitude at zero temperature. The evolution of

⁴ This may change when effects of the tensor interaction are included in the induced interaction.

the effective mass is included in the RG flow, as well as a simplified treatment of the renormalization of the quasiparticle strength. In the forward scattering limit, the role of the energy transfer is in the RG taken over by the cutoff in momentum space. We find that, in the long-wavelength limit, the dependence of the effective four-point vertex on Λ/q corresponds to the behavior with ω/q in the microscopic derivation of Fermi liquid theory by Landau.

Finally, we present the solution of the RG equations for neutron matter. These are obtained by employing the unique low momentum nucleon-nucleon interaction as the initial condition of the RG. Our results include the Fermi liquid parameters in the density range of interest for neutron stars as well as the full scattering amplitude for general (non-forward) scattering on the Fermi surface. Using the Fermi liquid parameters, we compute the equation of state, including polarization effects, by integrating the incompressibility [15]. Finally, we compute the $^1\text{S}_0$ superfluid pairing gap using weak coupling BCS theory. This is an application of our approach, which probes the angular dependence of the scattering amplitude. We generally find very good agreement with the results obtained in the polarization potential model by Ainsworth, Wambach and Pines [16,17]. However, it is worth noting that much of the model dependence, inherent in the work of Ainsworth *et al.*, can be avoided in the RG approach.

2 Renormalization group at one-loop

Shankar suggested that the relevant modes of a normal Fermi system may be isolated in a similar manner as for critical phenomena. In analogy with a Wilson-Kadanoff treatment of the latter [18], he proposed to separate the “slow” modes from the “fast”⁵ ones by imposing a cutoff around the Fermi surface [19]. Using a loop expansion, one can systematically generate the effective quasiparticle scattering amplitude and the effective quasiparticle interaction among slow quasiparticles and slow quasiholes at a given scale Λ .⁶ It has been shown that, in this approach, Fermi liquid theory emerges in the infrared limit when the cutoff is taken to zero [6,7,19,20,21,22,23,24,25].

Recently we derived the flow equations for the effective scattering amplitude and the quasiparticle interaction from the induced interaction of Babu and Brown [8]. In this paper, we employ the one-loop RG equations to compute

⁵ With “slow” we refer to the modes within a shell of width 2Λ centered around the Fermi momentum k_F , whereas the “fast” modes lie outside this shell.

⁶ The effective scattering amplitude at the scale Λ interpolates between the two-body irreducible interaction and the full scattering amplitude as described in the introduction.

the full scattering amplitude and the quasiparticle interaction on the Fermi surface starting from the vacuum two-body interaction. As we decimate down to the Fermi surface by letting $\Lambda \rightarrow 0$, we obtain not only the forward scattering amplitude for low-lying quasiparticle-quasihole excitations, but also the amplitude for general (non-forward) scattering processes of quasiparticles on the Fermi surface in the small momentum approximation.

In a loop expansion, the induced interaction corresponds to a summation of the direct and exchange particle-hole channels in a particular kinematic window, while loop contributions from the particle-particle (BCS) channel, are not summed by the RG equations derived in [8]. Thus, the contributions from the BCS channel should be included in the particle-hole irreducible driving term. In practice, one usually restricts oneself to the two-particle ladders with the bare nucleon-nucleon interaction (the Brueckner G matrix) or a simple generalization thereof, where the lowest order renormalization of the quasiparticle strength is included [10].

In the present work, we explore the one-loop truncation of the RG equations. When only one channel is considered, the one-loop RG equation is exact in the sense that it is equivalent to the corresponding scattering equation. When both the direct and exchange channels are included, the scattering amplitude remains antisymmetric under the RG flow. Calculations with the induced interaction for liquid ^3He and nuclear matter show that the systematic inclusion of exchange channel contributions is crucial for obtaining a realistic description of the effective interaction [9,10,11,26,27,28,29]. Therefore, we expect the one-loop RG to capture the essential physics of the soft modes near the Fermi surface. In this approximation, our RG equations are equivalent to those obtained previously by Dupuis [20].

The two one-loop particle-hole contributions to the effective four-point function are shown in Fig. 1, where the integration is restricted to a fast particle and a fast hole. The effective four-point vertex γ depends on three momentum variables, the cutoff and the energy transfer ω in the zero sound channel,⁷

$$\gamma = \gamma((\omega, \mathbf{q}), \mathbf{q}', \mathbf{p} + \mathbf{p}'; \Lambda), \quad (1)$$

where $\mathbf{q}' = \mathbf{p} - \mathbf{p}'$. Under exchange, the momentum transfer \mathbf{q} and \mathbf{q}' have to be interchanged, whereas the particle-pair momentum $\mathbf{p} + \mathbf{p}'$ remains invariant. We note that in the limit $|\mathbf{q}| \rightarrow 0$, the scattering amplitude describes long-wavelength excitations in the zero sound channel, while $|\mathbf{p} + \mathbf{p}'| \rightarrow 0$

⁷ For energy-independent initial conditions, one can set the energy transfers ω and ω' to zero in the RG equations. Here we retain only the ω for the purpose of discussing the limits $\omega/q \rightarrow 0$ and $q/\omega \rightarrow 0$. The role of ω for the purpose of obtaining the forward scattering amplitude and the quasiparticle interaction is then taken over by the cutoff Λ , as we will show in the next section.

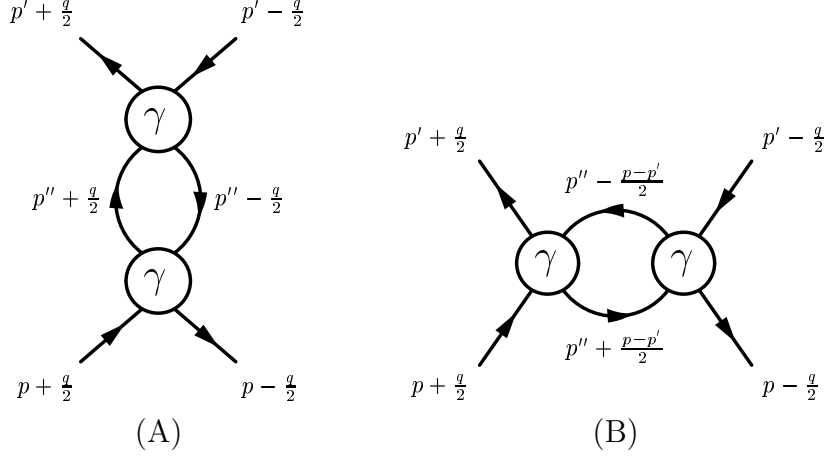


Fig. 1. The one-loop contributions to the RG equation. (A): The zero sound (ZS) channel with momentum transfer \mathbf{q} and (B): the exchange channel (ZS') with momentum transfer \mathbf{q}' . (Our convention for the momentum flow is in the direction of the particle and hole arrows.) As defined in the text, γ denotes the effective four-point vertex.

corresponds to the BCS pairing singularity.

We define the effective quasiparticle interaction $f(\mathbf{q}'; \Lambda)$ at the scale Λ by the limit

$$f(\mathbf{q}'; \Lambda) = \lim_{\omega \rightarrow 0} \gamma((\omega, \mathbf{q} = 0), \mathbf{q}', \mathbf{p} + \mathbf{p}'; \Lambda), \quad (2)$$

and the effective quasiparticle scattering amplitude, extended to finite momentum transfer \mathbf{q} , by

$$a(\mathbf{q}, \mathbf{q}'; \Lambda) = \gamma((\omega = 0, \mathbf{q}), \mathbf{q}', \mathbf{p} + \mathbf{p}'; \Lambda). \quad (3)$$

In order to allow a proper treatment of the momentum dependence in the exchange channel, we generalize the effective interaction $f(\mathbf{q}'; \Lambda)$ to finite \mathbf{q} , $f(\mathbf{q}, \mathbf{q}'; \Lambda)$, keeping in mind that the Landau quasiparticle interaction is obtained for $|\mathbf{q}| = 0$.

The RG equations at one-loop and zero temperature are given by [8]

$$\begin{aligned} \frac{d}{d\Lambda} a(\mathbf{q}, \mathbf{q}'; \Lambda) = & z_{k_F}^2 \frac{d}{d\Lambda} \left\{ g \int_{\text{fast}, \Lambda} \frac{d^3 \mathbf{p}''}{(2\pi)^3} \frac{n_{\mathbf{p}''+\mathbf{q}/2} - n_{\mathbf{p}''-\mathbf{q}/2}}{\varepsilon_{\mathbf{p}''+\mathbf{q}/2} - \varepsilon_{\mathbf{p}''-\mathbf{q}/2}} \right\} \\ & \times a\left(\mathbf{q}, \frac{\mathbf{p} + \mathbf{p}'}{2} + \frac{\mathbf{q}'}{2} - \mathbf{p}''; \Lambda\right) a\left(\mathbf{q}, \mathbf{p}'' - \frac{\mathbf{p} + \mathbf{p}'}{2} + \frac{\mathbf{q}'}{2}; \Lambda\right) \\ & + \frac{d}{d\Lambda} f(\mathbf{q}, \mathbf{q}'; \Lambda) \end{aligned} \quad (4)$$

$$\begin{aligned} \frac{d}{d\Lambda} f(\mathbf{q}, \mathbf{q}'; \Lambda) = & -z_{k_F}^2 \frac{d}{d\Lambda} \left\{ g \int_{\text{fast}, \Lambda} \frac{d^3 \mathbf{p}''}{(2\pi)^3} \frac{n_{\mathbf{p}''+\mathbf{q}'/2} - n_{\mathbf{p}''-\mathbf{q}'/2}}{\varepsilon_{\mathbf{p}''+\mathbf{q}'/2} - \varepsilon_{\mathbf{p}''-\mathbf{q}'/2}} \right\} \\ & \times a\left(\mathbf{q}', \frac{\mathbf{p} + \mathbf{p}'}{2} + \frac{\mathbf{q}}{2} - \mathbf{p}''; \Lambda\right) a\left(\mathbf{q}', \mathbf{p}'' - \frac{\mathbf{p} + \mathbf{p}'}{2} + \frac{\mathbf{q}}{2}; \Lambda\right), \end{aligned} \quad (5)$$

where g denotes the spin-isospin degeneracy, for neutron matter $g = 2$, and z_{k_F} is the quasiparticle strength at the Fermi surface. The effective scattering amplitude includes contributions from both the ZS and ZS' channel, whereas for the effective interaction only the exchange contribution, which corresponds to the induced interaction [5], remains. The vertices in the one-loop diagrams are given by the scattering amplitude at the current scale. Consequently, the renormalization due to the fast modes in both particle-hole channels is included. Furthermore, since we will employ the unique, energy-independent low momentum nucleon-nucleon interaction of Bogner *et al.* [13,14] as initial condition of the RG flow, we have set the energy transfer to zero, in particular $\omega = 0$, in the above RG equations. Note that the derivatives with respect to Λ on the right hand side of Eqs. (4,5) act only on the phase space factors. Furthermore, in order not to overload the equations, we have suppressed the spin variables. They will be discussed in detail below. It is apparent that the RG equation, Eq. (4), preserves the antisymmetry of the scattering amplitude under the RG flow. Hence, the Pauli principle sum rules [3,30] are automatically fulfilled for the resulting Fermi liquid parameters.

As motivated in the introduction, we evaluate the one-loop beta functions in the long-wavelength approximation. Obviously, the phase space for the intermediate particle-hole pair in the ZS channel is open for $\Lambda < q/2$, where q denotes $|\mathbf{q}|$, with an analogous expression for the ZS' channel, see Fig. 2. For small q, q' , the integration over \mathbf{p}'' in the beta functions reduces to an integration over a solid angle on the Fermi surface. We find for the RG equations at

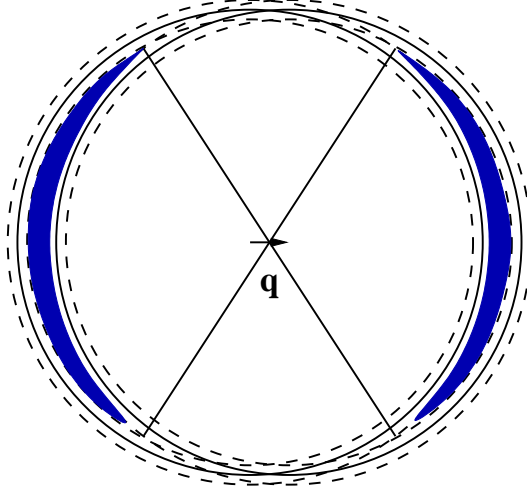


Fig. 2. The phase-space factors in the RG equation, Eq. (4), are non-zero in the filled areas. The dashed circles denote the cutoff around the Fermi surfaces.

zero temperature⁸

$$\Lambda \frac{d}{d\Lambda} a(\mathbf{q}, \mathbf{q}'; \Lambda) = \Theta(q - 2\Lambda) \beta_{\text{ZS}}[a, \mathbf{q}, \Lambda] - \Theta(q' - 2\Lambda) \beta_{\text{ZS}}[a, \mathbf{q}', \Lambda] \quad (6)$$

$$\begin{aligned} &= \Theta(q - 2\Lambda) z_{k_F}^2 \frac{2\Lambda}{q} N(\Lambda) \\ &\times \int_{2\Lambda/q < |\cos(\theta_{\mathbf{p}''\mathbf{q}})| < 1} \frac{d\Omega_{\mathbf{p}''}}{4\pi} \frac{\text{sign}(\cos(\theta_{\mathbf{p}''\mathbf{q}}))}{\cos(\theta_{\mathbf{p}''\mathbf{q}})} \\ &\times a\left(\mathbf{q}, \frac{\mathbf{p} + \mathbf{p}'}{2} + \frac{\mathbf{q}'}{2} - \mathbf{p}''; \Lambda\right) a\left(\mathbf{q}, \mathbf{p}'' - \frac{\mathbf{p} + \mathbf{p}'}{2} + \frac{\mathbf{q}'}{2}; \Lambda\right) \\ &- \Theta(q' - 2\Lambda) z_{k_F}^2 \frac{2\Lambda}{q'} \{\mathbf{q} \leftrightarrow \mathbf{q}'\} \end{aligned} \quad (7)$$

$$\begin{aligned} \Lambda \frac{d}{d\Lambda} f(\mathbf{q}, \mathbf{q}'; \Lambda) &= -\Theta(q' - 2\Lambda) z_{k_F}^2 \frac{2\Lambda}{q'} N(\Lambda) \\ &\times \int_{2\Lambda/q' < |\cos(\theta_{\mathbf{p}''\mathbf{q}'})| < 1} \frac{d\Omega_{\mathbf{p}''}}{4\pi} \frac{\text{sign}(\cos(\theta_{\mathbf{p}''\mathbf{q}'}))}{\cos(\theta_{\mathbf{p}''\mathbf{q}'})} \\ &\times a\left(\mathbf{q}', \frac{\mathbf{p} + \mathbf{p}'}{2} + \frac{\mathbf{q}}{2} - \mathbf{p}''; \Lambda\right) a\left(\mathbf{q}', \mathbf{p}'' - \frac{\mathbf{p} + \mathbf{p}'}{2} + \frac{\mathbf{q}}{2}; \Lambda\right). \end{aligned} \quad (8)$$

The factor $N(\Lambda) = g m^*(\Lambda) k_F / 2\pi^2$ denotes the density of states at the Fermi surface. The effective mass is determined self-consistently from the effective

⁸ Contrary to statements in the literature, the RG equations at zero temperature are very transparent. The δ functions appearing in the beta function can be handled in a straightforward manner and the phase space integrals can in fact be evaluated analytically. A non-zero temperature introduces a further scale, which competes with the cutoff and consequently must be treated with special care.

interaction

$$\frac{m^*(\Lambda)}{m} = \frac{1}{1 - f_1(\Lambda) \frac{g m k_F}{6 \pi^2}}. \quad (9)$$

This enforces Galilean invariance on the system. The effective mass is continuously adapted as the flow equations are integrated towards the Fermi surface. In Eq. (9), $f_1(\Lambda)$ is given by the projection of the quasiparticle interaction on the $l = 1$ Legendre polynomial. If one restricts the analysis to the ZS channel and assumes that the Fermi liquid parameters are given, the solution of the flow equation reproduces the relations between the quasiparticle interaction and the forward scattering amplitude. In the appendix we give a detailed derivation of the beta function in Eqs. (6-8) and the solution of the RG equation in the ZS channel.

For $\Lambda \geq k_F$, the particle-hole contributions vanish in the momentum range of interest $q, q' \leq 2k_F$ (see the explicit expressions given in the appendix). Hence, we can start the decimation at $\Lambda_0 = k_F$ with a particle-hole irreducible boundary condition on the RG equations, Eqs. (7,8). This boundary condition may be identified with the direct interaction of [5]. We approximate the direct interaction with the vacuum two-body low momentum interaction $V_{\text{low } k}$ at a cutoff scale $\Lambda_{V_{\text{low } k}} = \sqrt{2}k_F$, which will be motivated in Section 4. This choice of the cutoff approximately accounts for the Pauli blocking of intermediate states in the BCS channel, which suppresses large structures, like the quasi bound state in the 1S_0 channel and tames the short-range repulsion of the nucleon-nucleon interaction. Since, in isotriplet channels, $V_{\text{low } k}$ is almost independent of the cutoff over a large range, the precise value of $\Lambda_{V_{\text{low } k}}$ is not crucial. Furthermore, we allow for a minimal in medium correction of the starting values, in terms of the renormalization of the quasiparticle strength z_{k_F} . To a certain extent this accounts for the contribution of higher order particle-hole irreducible diagrams to the direct interaction [10]. At the initial cutoff Λ_0 , we thus have

$$a(\mathbf{q}, \mathbf{q}'; \Lambda_0) = f(\mathbf{q}, \mathbf{q}'; \Lambda_0) = \gamma_{\text{vacuum}}(\mathbf{q}, \mathbf{q}'), \quad (10)$$

where $\gamma_{\text{vacuum}}(\mathbf{q}, \mathbf{q}')$ will be specified below. We solve the RG flow with two different assumptions for the z_{k_F} factor. In one case, we will use a static, density-independent mean value of $z_{k_F}^2 = 0.9$, which remains unchanged under the RG. In the other case, we compute the z_{k_F} factor dynamically, by assuming that the change of the effective mass from the initial one, owing to the direct interaction, is due to the z_{k_F} factor alone. We then adjust the factor $z_{k_F}^2$ in the RG equations, Eqs. (7,8), self-consistently as we decimate to the Fermi surface, i.e., we start with $z_{k_F}(\Lambda_0) = 1$ and change the z_{k_F} factor according to

$$\frac{1}{z_{k_F}(\Lambda)} = \frac{m^*(\Lambda)}{m^*(\Lambda_0)}. \quad (11)$$

In this approximation we account for the momentum dependence of the self-energy corresponding to the direct interaction in $m^*(\Lambda_0)$ and make the rea-

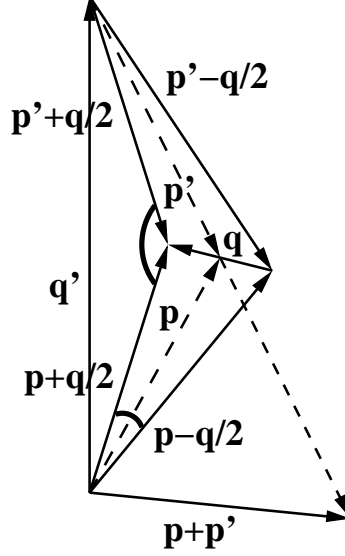


Fig. 3. The configuration of quasiparticles and quasiholes on the Fermi surface. The arcs denote the angles $\theta_{\mathbf{q}}$ and $\theta_{\mathbf{q}'}$ opposite of \mathbf{q} and \mathbf{q}' , respectively.

sonable assumption that the modification of the effective mass due to the induced interaction is dominated by the energy dependence of the self energy, the so called E -mass [31]. We shall see later that this approximation leads to a z_{k_F} factor in rather good agreement with Brueckner-Hartree-Fock calculations [32,33] at intermediate Fermi momenta $0.5 \text{ fm}^{-1} < k_F < 1.5 \text{ fm}^{-1}$.

Finally, we assume that the interacting particles are on the Fermi surface. The momentum variables \mathbf{q} , \mathbf{q}' and $\mathbf{p} + \mathbf{p}'$ then form an orthogonal set of basis vectors, which follows straightforwardly from the conditions $|\mathbf{p} \pm \mathbf{q}/2| = k_F$ and $|\mathbf{p}' \pm \mathbf{q}/2| = k_F$. Our geometry is shown in Fig. 3, where $\theta_{\mathbf{q}}$ and $\theta_{\mathbf{q}'}$ denote the angles between $\mathbf{p} + \mathbf{q}/2$, $\mathbf{p} - \mathbf{q}/2$ and $\mathbf{p} + \mathbf{q}/2$, $\mathbf{p}' + \mathbf{q}/2$ respectively and are related to the momentum transfer by means of⁹

$$q = 2 k_F \sin \frac{\theta_{\mathbf{q}}}{2} \quad (12)$$

$$q' = 2 k_F \sin \frac{\theta_{\mathbf{q}'}}{2} \quad (13)$$

$$|\mathbf{p} + \mathbf{p}'| = 2 k_F \sqrt{\frac{\cos \theta_{\mathbf{q}} + \cos \theta_{\mathbf{q}'}}{2}}. \quad (14)$$

The orthogonality of the coordinate system is very convenient for the numerical implementation, in particular for the evaluating the arguments of the scattering amplitude in the beta functions. Given this geometry, the scatter-

⁹ Our definition of $\theta_{\mathbf{q}'}$ differs from the angle θ_L between the momenta \mathbf{p} and \mathbf{p}' employed by Ainsworth and Bedell [29]. The relation between the two angles is given by $2 \cos \theta_{\mathbf{q}'} = 1 - \cos \theta_{\mathbf{q}} + (1 + \cos \theta_{\mathbf{q}}) \cos \theta_L$.

ing amplitude depends only on the magnitude of the two momentum transfers q and q' . Under the restriction that the momenta of the quasiparticles are constrained to the Fermi surface, we have $q^2 + q'^2 \leq 4k_F^2$ or equivalently $\cos\theta_{\mathbf{q}} + \cos\theta_{\mathbf{q}'} \geq 0$.

The beta functions involve scattering to fast particle-hole intermediate states away from the Fermi surface. In the coordinate system shown in Fig. 3 one finds

$$\mathbf{p} = k_F \cos \frac{\theta_{\mathbf{q}}}{2} \hat{\mathbf{p}} \quad (15)$$

$$\mathbf{p}' = k_F \cos \frac{\theta_{\mathbf{q}}}{2} \hat{\mathbf{p}}'. \quad (16)$$

Using these relations we obtain, for small q , where $\hat{\mathbf{p}} \cdot \hat{\mathbf{p}}' \approx \cos\theta_{\mathbf{q}'}$, the approximate expression

$$|\mathbf{p} + \mathbf{p}'| = 2k_F \cos \frac{\theta_{\mathbf{q}}}{2} \cos \frac{\theta_{\mathbf{q}'}}{2}, \quad (17)$$

which allows us to smoothly extend the RG flow to $q^2 + q'^2 > 4k_F^2$, where Eq. (14) is not useful.

3 The forward scattering limit in the RG and the inclusion of spin

At the one-loop level, the solution of the RG flow in the particle-hole channels is particularly transparent and involves only the effective scattering amplitude. The quasiparticle interaction at arbitrary cutoff is simply given by the $q = 0$ values of the scattering amplitude,

$$\frac{d}{d\Lambda} f(q = 0, \mathbf{q}'; \Lambda) = \frac{d}{d\Lambda} a(q = 0, \mathbf{q}'; \Lambda). \quad (18)$$

In Fermi liquid theory, the singularity in the ZS channel can be used to eliminate the quasiparticle-quasihole contributions in this channel by taking the limit $q/\omega \rightarrow 0$. For an energy-independent RG flow, the role of ω is taken over by the cutoff. In the RG equation, Eq. (7), the ZS contribution can be explicitly eliminated by setting q to zero (see also Fig. 2, where the contributions from a fast particle and a fast hole are absent for $q = 0$). Therefore, the forward scattering limits in Fermi Liquid Theory (FLT) are in the RG approach at zero temperature obtained by

$$f_{\text{FLT}}(\mathbf{q}') = \lim_{\Lambda \rightarrow 0} a(q = 0, \mathbf{q}'; \Lambda) \quad (19)$$

$$a_{\text{FLT}}(\mathbf{q}') = \lim_{q \rightarrow 0} a(\mathbf{q}, \mathbf{q}'; \Lambda = 0). \quad (20)$$

This is analogous to the $q/\omega \rightarrow 0$ and $\omega/q \rightarrow 0$ limits in Fermi liquid theory. The forward scattering amplitude and the Fermi liquid quasiparticle interaction are obtained as stable solutions of the RG equation, Eq. (7), as the cutoff is taken to zero. We note that the beta functions explicitly depend on the cutoff and the momentum transfer in the particular channel. In fact, $\Lambda \frac{d}{d\Lambda} a(\mathbf{q}, \mathbf{q}'; \Lambda)$ is proportional to the cutoff itself, and thus the beta functions vanish by construction as the cutoff is taken to zero. From the definition of the quasiparticle interaction, Eq. (19), we observe that the Fermi liquid parameters depend in a nontrivial fashion on the effective scattering amplitude.

The inclusion of spin is straightforward. The RG equation for the scattering amplitude, $a(\mathbf{q}, \mathbf{q}'; \Lambda) + b(\mathbf{q}, \mathbf{q}'; \Lambda) \boldsymbol{\sigma} \cdot \boldsymbol{\sigma}'$, is given by

$$\begin{aligned} \Lambda \frac{d}{d\Lambda} (a + b \boldsymbol{\sigma} \cdot \boldsymbol{\sigma}') = & \Theta(q - 2\Lambda) \left\{ \beta_{\text{ZS}}[a, \mathbf{q}, \Lambda] + \beta_{\text{ZS}}[b, \mathbf{q}, \Lambda] \boldsymbol{\sigma} \cdot \boldsymbol{\sigma}' \right\} \\ & - \Theta(q' - 2\Lambda) \left\{ \frac{1}{2} \beta_{\text{ZS}'}[a, \mathbf{q}', \Lambda] + \frac{3}{2} \beta_{\text{ZS}'}[b, \mathbf{q}', \Lambda] \right\} \\ & - \Theta(q' - 2\Lambda) \left\{ \frac{1}{2} \beta_{\text{ZS}'}[a, \mathbf{q}', \Lambda] - \frac{1}{2} \beta_{\text{ZS}'}[b, \mathbf{q}', \Lambda] \right\} \boldsymbol{\sigma} \cdot \boldsymbol{\sigma}', \end{aligned} \quad (21)$$

where the coefficients in Eq. (21) are the recoupling coefficients generated by the spin exchange operator (see [8]). In [34], the RG flow is illustrated for a schematic model of spin polarized fermions.

4 Results

We initialize the RG flow with the unique low momentum nucleon-nucleon interaction $V_{\text{low } k}$ of Bogner *et al.* [13,14]. This is derived from realistic nucleon-nucleon potentials, such as the Bonn, Paris, Argonne and Nijmegen interactions, by integrating out the high momentum modes while preserving the half-on-shell T matrix and consequently the experimental phase shifts. In $V_{\text{low } k}$ the short-range repulsion has been tamed. Therefore, it is possible to perform many-body calculations directly with $V_{\text{low } k}$ without first computing the Brueckner G matrix. In fact, for $\Lambda_{V_{\text{low } k}} \sim k_F$, $V_{\text{low } k}$ exhibits many of the salient features of the G matrix [8].

In the case of a static, cutoff independent z_{k_F} factor, a minimal in medium correction to the direct interaction is, as discussed above, included by multiplying $V_{\text{low } k}$ by $z_{k_F}^2$ from the start of the RG. After projecting out the non-central components, the direct and exchange contribution are in a partial wave basis

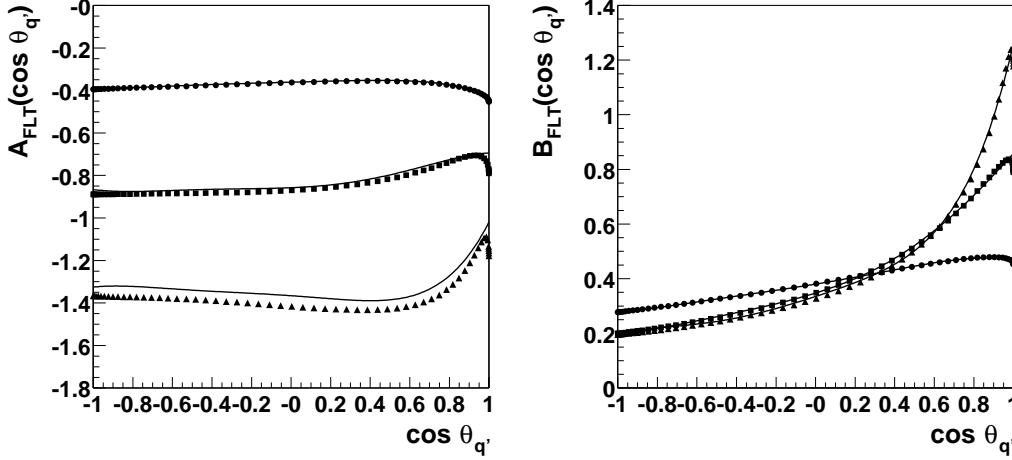


Fig. 4. The comparison of the RG solution for the forward scattering amplitude $A_{\text{FLT}}(\cos \theta_{\mathbf{q}'})$ and $B_{\text{FLT}}(\cos \theta_{\mathbf{q}'})$ (points) to that obtained from the corresponding quasiparticle interaction (The solid lines include the Fermi liquid parameters up to $l \leq 5$). The solutions given are for the adaptive z_{k_F} factor and a density corresponding to $k_F = 0.6 \text{ fm}^{-1}$ (dots), $k_F = 1.0 \text{ fm}^{-1}$ (squares) and $k_F = 1.35 \text{ fm}^{-1}$ (triangles). Similar agreement is found at other densities. The average momentum grid spacing is $\Delta q/k_F = \Delta q'/k_F = 0.033$.

given by

$$\begin{aligned}
 \langle S | \mathcal{A}(\mathbf{q}, \mathbf{q}'; \Lambda_0) | S \rangle &= z_{k_F}^2(\Lambda_0) N(\Lambda_0) \frac{4\pi}{2S+1} \sum_{J,l} (2J+1) \left(1 - (-1)^{l+S+1}\right) \\
 &\times \left\langle \frac{|\mathbf{q}' - \mathbf{q}|}{2} \middle| l S J T = 1 \middle| V_{\text{low k}} \middle| \frac{|\mathbf{q}' + \mathbf{q}|}{2} \middle| l S J T = 1 \right\rangle \\
 &\times P_l \left(\frac{(\mathbf{q}' + \mathbf{q}) \cdot (\mathbf{q}' - \mathbf{q})}{|\mathbf{q}' + \mathbf{q}| |\mathbf{q}' - \mathbf{q}|} \right), \tag{22}
 \end{aligned}$$

where we set $T = 1$ for neutron matter and P_l denotes the Legendre polynomial of degree l . We include all partial waves up to $J \leq 6$ in the driving term. Furthermore, we have introduced the dimensionless scattering amplitude \mathcal{A} by means of

$$\begin{aligned}
 \mathcal{A}(\mathbf{q}, \mathbf{q}'; \Lambda) &= A(\mathbf{q}, \mathbf{q}'; \Lambda) + B(\mathbf{q}, \mathbf{q}'; \Lambda) \boldsymbol{\sigma} \cdot \boldsymbol{\sigma}' \\
 &= z_{k_F}^2(\Lambda) N(\Lambda) \left(a(\mathbf{q}, \mathbf{q}'; \Lambda) + b(\mathbf{q}, \mathbf{q}'; \Lambda) \boldsymbol{\sigma} \cdot \boldsymbol{\sigma}' \right). \tag{23}
 \end{aligned}$$

In the scattering geometry discussed in the previous section, \mathbf{q} and \mathbf{q}' are orthogonal, and thus the magnitude of the relative momentum in the initial and final states are both given by

$$\frac{|\mathbf{q}' \pm \mathbf{q}|}{2} = \frac{\sqrt{q'^2 + q^2}}{2}. \tag{24}$$

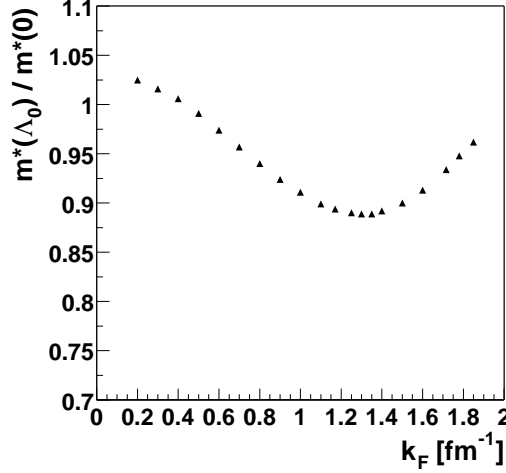


Fig. 5. The ratio of the direct to the full effective mass $m^*(\Lambda_0)/m^*(\Lambda = 0)$, which we use as a running z_{k_F} factor in the RG equation, versus Fermi momentum k_F .

Let us now discuss the choice of the cutoff in the direct interaction, $\Lambda_{V_{\text{low } k}}$. In [8] we argued that for the scattering of two particles with total momentum $\mathbf{p} + \mathbf{p}' = 0$ relative to the Fermi sea, the choice $\Lambda_{V_{\text{low } k}} = k_F$ accounts for the Pauli blocking of the intermediate states. For non-zero total momenta, the effect of Pauli blocking is on the average more severe. The Pauli blocking factor, averaged over the total momentum of two particles on the Fermi surface, corresponds to an angular averaged cutoff of $\simeq 1.5 k_F$. We choose the cutoff for the low momentum nucleon-nucleon interaction at $\Lambda_{V_{\text{low } k}} = \sqrt{2} k_F$.¹⁰ This choice has two additional somewhat technical advantages. First, inspection of the flow equations, Eqs. (4,5), reveals that momentum transfers up to $k_{\text{max}} = \sqrt{5} k_F/2$ are needed to scatter to intermediate states away from the Fermi surface. Since $V_{\text{low } k}$ is defined only for momenta less than the cutoff, one would like to have $k_{\text{max}} < \Lambda_{V_{\text{low } k}}$ in a consistent description. Second, a cutoff $\Lambda_{V_{\text{low } k}} = \sqrt{2} k_F$ allows one to define the scattering amplitude continuously on the momentum grid $q, q' \leq 2 k_F$.

The numerical procedure for solving the RG equations, Eq. (7) or Eq. (21), may be checked in the following way. First, the antisymmetry of the effective scattering amplitude is by construction preserved under the RG

$$\frac{d}{d\Lambda} \langle S = 1 | \mathcal{A}(\mathbf{q}, \mathbf{q}'; \Lambda) + \mathcal{A}(\mathbf{q}', \mathbf{q}; \Lambda) | S = 1 \rangle = 0. \quad (25)$$

Furthermore, the Fermi liquid quasiparticle interaction and the forward scattering amplitude, Eqs. (19,20), must satisfy general relations of Fermi liquid theory. The Fermi liquid parameters are given by the projection of the quasi-

¹⁰ Since the cutoff dependence of $V_{\text{low } k}$ is very weak for $\Lambda > 0.7 \text{ fm}^{-1}$ [14], the exact value of $\Lambda_{V_{\text{low } k}}$ is not decisive.

particle interaction on Legendre polynomials

$$\mathcal{F}_{\text{FLT}}(\cos \theta_{\mathbf{q}'}) = z_{k_F}^2(0) N(0) f_{\text{FLT}}(\mathbf{q}') = \sum_l (F_l + G_l \boldsymbol{\sigma} \cdot \boldsymbol{\sigma}') P_l(\cos \theta_{\mathbf{q}'}), \quad (26)$$

where $\theta_{\mathbf{q}'}$ is the angle between the quasiparticle momenta \mathbf{p} and \mathbf{p}' in the limit $q = 0$. Similarly, the forward scattering amplitude is expanded in Legendre polynomials

$$\mathcal{A}_{\text{FLT}}(\cos \theta_{\mathbf{q}'}) = \sum_l (A_l + B_l \boldsymbol{\sigma} \cdot \boldsymbol{\sigma}') P_l(\cos \theta_{\mathbf{q}'}). \quad (27)$$

The forward scattering amplitude is related to the Fermi liquid parameters through [3]

$$A_l = \frac{F_l}{1 + F_l/(2l + 1)} \quad (28)$$

$$B_l = \frac{G_l}{1 + G_l/(2l + 1)}. \quad (29)$$

These relations are fulfilled by our numerical solution with an accuracy of the order of $\Delta q/k_F$ and $\Delta q'/k_F$, where Δq and $\Delta q'$ are the momentum grid spacings in q and q' respectively. In Fig. 4 we compare the numerical RG solution for the forward scattering amplitude to that obtained from the corresponding quasiparticle interaction using these relations, Eqs. (28,29). The antisymmetry of the scattering amplitude is preserved with machine precision.

We start the discussion of the numerical results by presenting the change of the effective mass, i.e., the ratio of the effective mass obtained from the direct interaction to the full effective mass. The ratio $m^*(\Lambda_0)/m^*(\Lambda)$ is taken as an approximation to the running z_{k_F} factor in the RG flow. The final value $m^*(\Lambda_0)/m^*(\Lambda = 0)$ is shown in Fig. 5. For Fermi momenta $1.0 \text{ fm}^{-1} < k_F < 1.5 \text{ fm}^{-1}$, this approximation agrees well with the values obtained in Brueckner-Hartree-Fock calculations including rearrangement terms, as reported by Zuo *et al.* [32]. At lower densities, $0.5 \text{ fm}^{-1} < k_F < 1.0 \text{ fm}^{-1}$, the agreement is qualitatively good, but we find a somewhat smaller value of the z_{k_F} factor compared with the results of Baldo and Grasso [33]. We notice that, for densities below $k_F = 0.5 \text{ fm}^{-1}$, this procedure yields a quasiparticle strength slightly larger than one, while above 1.5 fm^{-1} , the resulting z_{k_F} increases with density. The increase of z_{k_F} with density cannot be excluded from first principles, but seems unlikely. Thus, we conclude that our simple procedure seems to work reasonably well in the density range $0.5 \text{ fm}^{-1} < k_F < 1.5 \text{ fm}^{-1}$. However, outside this range, corrections due to e.g., rearrangement terms, are probably needed. In this paper, our emphasis is on particle-hole polarization effects.

4.1 The Fermi liquid parameters and the scattering amplitude at finite q

In Fig. 6 we show our results for the $l = 0$ and $l = 1$ Fermi liquid parameters as functions of the Fermi momentum. Since the RG flow is antisymmetric by construction, the Fermi liquid parameters obey the Pauli principle sum rules [3,30]. The low momentum interaction drives the flow in the ZS' channel for the quasiparticle interaction, and thus our results include effects of the induced interaction of Babu and Brown.¹¹ A further advantage of the RG approach is that the calculations can be performed without truncating the expansion of the quasiparticle interaction, Eq. (26), at some l .

Generally, we find a very good agreement between our results¹² and the ones obtained using the polarization potential model by Ainsworth, Wambach and Pines [16,17]. There are minor differences in the value of the effective mass, which is treated self-consistently in the RG approach. We note that, in the density range $0.6 \text{ fm}^{-1} < k_F < 1.4 \text{ fm}^{-1}$, we find that the effective mass at the Fermi surface exceeds unity. The quasiparticle interaction was also calculated previously using the induced interaction in [27,35,36]. In these papers, the value for the $l = 0$ spin-dependent parameter G_0 is in good agreement with ours, while for the spin-independent F_0 , there are differences. We stress the important role of the large G_0 for the induced interaction. This Landau parameter causes the strong spin-density correlations, which in turn enhance the Landau parameter F_0 and consequently the incompressibility of neutron matter.

The results can be qualitatively understood by inspecting the RG equation for the quasiparticle interaction, Eq. (21) for $q = 0$,

$$\Lambda \frac{d}{d\Lambda} a(q = 0, \mathbf{q}'; \Lambda) = -\Theta(q' - 2\Lambda) \left\{ \frac{1}{2} \beta_{\text{ZS}'}[a, \mathbf{q}', \Lambda] + \frac{3}{2} \beta_{\text{ZS}'}[b, \mathbf{q}', \Lambda] \right\} \quad (30)$$

$$\Lambda \frac{d}{d\Lambda} b(q = 0, \mathbf{q}'; \Lambda) = -\Theta(q' - 2\Lambda) \left\{ \frac{1}{2} \beta_{\text{ZS}'}[a, \mathbf{q}', \Lambda] - \frac{1}{2} \beta_{\text{ZS}'}[b, \mathbf{q}', \Lambda] \right\}. \quad (31)$$

In this qualitative argument we can neglect Fermi liquid parameters with $l \geq 1$. At a typical Fermi momentum $k_F = 1.0 \text{ fm}^{-1}$, we observe that the initial F_0 and G_0 are similar in absolute value, $|F_0| \approx |G_0| \approx 0.8$. Consequently, there

¹¹ By analyzing the RG equations in [8], one finds that the one-loop RG generates a subset of the particle-hole parquet diagrams. The diagrams that are missed correspond to terms, where the renormalization is due to integrating out internal lines of the vertex functions γ in Fig. 1. In the parquet equations, they correspond to certain diagrams involving left or right vertex corrections in the direct or exchange particle-hole channel.

¹² We note that at large Fermi momenta a smaller z_{k_F} factor, as discussed above, would lead to an overall decrease of the magnitude of the Fermi liquid parameters.

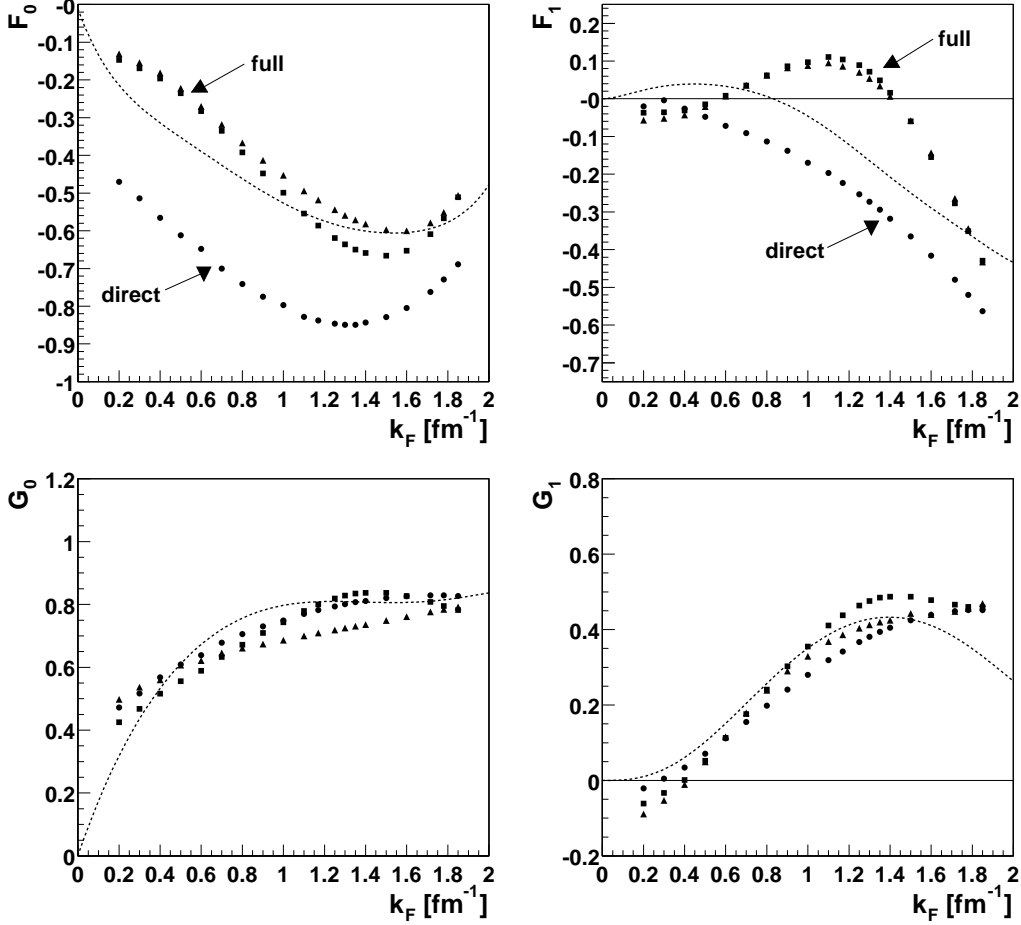


Fig. 6. The $l = 0$ and $l = 1$ Fermi liquid parameters versus the Fermi momentum k_F . The dots denote the direct contribution only ($z_{k_F} = 1$, but including the effective mass in the density of states), whereas the squares (constant z_{k_F} factor) and the triangles (adaptive z_{k_F} factor) are calculated from the full RG solution. The results of Wambach *et al.* [17] are given for comparison as dashed lines.

is a cancellation between the contributions due to the spin-independent and spin-dependent parameters in Eq. (31), while in Eq. (30) both contributions are repulsive. Thus, one expects a relatively small effect of the RG flow on G_0 and a substantial renormalization of F_0 , in agreement with our results.

The approximate relationship for the z_{k_F} factor, Eq. (11), is reasonable, if there is a strong frequency dependence of the polarization contributions to the nucleon self-energy. This may be the case if one of the Fermi liquid parameters is strongly attractive [37]. In the density range where we obtain a reasonable z_{k_F} factor, F_0 is indeed most negative.

The RG approach enables us to compute the scattering amplitude for general scattering processes on the Fermi surface, without making further assumptions for the dependence upon the particle-hole momentum transfers q and

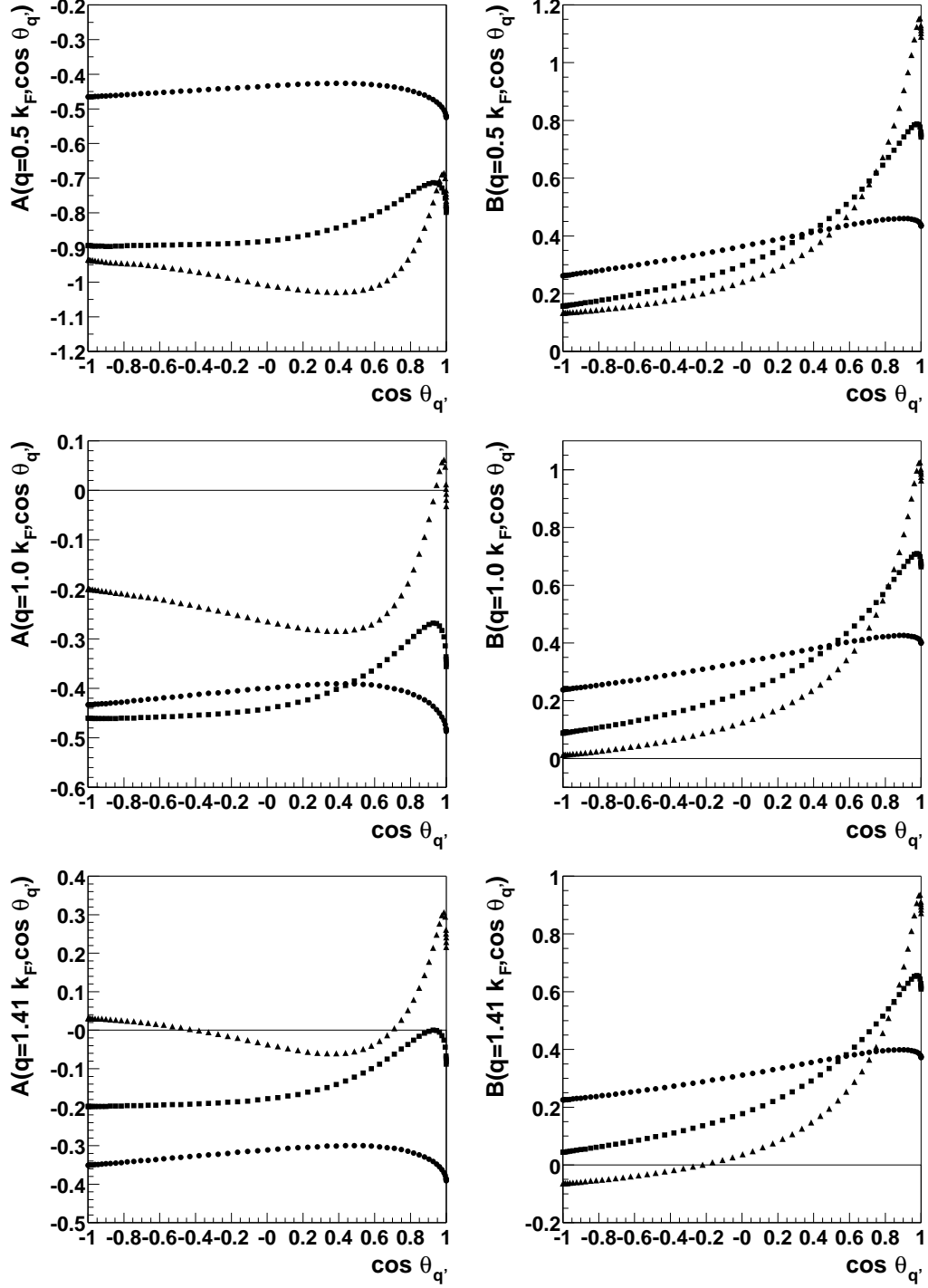


Fig. 7. The RG solution for the scattering amplitude on the Fermi surface $A(\mathbf{q}, \mathbf{q}')$ and $B(\mathbf{q}, \mathbf{q}')$ versus $\cos \theta_{q'}$ for different cuts at finite momentum transfer $q = 0.5, 1.0$ and $\sqrt{2} k_F$. The RG flow is solved with the adaptive z_{k_F} factor for different densities, $k_F = 0.6 \text{ fm}^{-1}$ (dots), $k_F = 1.0 \text{ fm}^{-1}$ (squares) and $k_F = 1.35 \text{ fm}^{-1}$ (triangles).

q' . In Fig. 7, we show the full scattering amplitude for different values of the momentum transfer q and different densities. We recall that for scattering on

the Fermi surface the exchange momenta are restricted to $q^2 + q'^2 \leq 4 k_F^2$. The scattering amplitude at finite momentum transfer is of great interest for calculating transport processes and for assessing the consequences of superfluidity in neutron stars.

4.2 The 1S_0 superfluid gap

It has been discussed by several authors that polarization effects, which are necessary in order to satisfy the Pauli principle in microscopic calculations, have a profound influence on superfluidity in neutron stars [16,17,38,39]. A reduction of the pairing gap due to polarization effects was first found by Clark *et al.* [38]. Subsequently, Ainsworth, Wambach and Pines explored particle-hole polarization effects in detail, using the framework of the induced interaction [5] combined with the polarization potential model [16,17]. They found a large reduction of the 1S_0 superfluid gap from a maximum gap of 5 MeV to 0.9 MeV, when the induced interaction was included. A reduction to similar magnitude was obtained by Chen *et al.* in a variational calculation, when CBF correlations were included [40,41]. Recently, Schulze *et al.* also found a substantial reduction of the gap by employing a phase-space averaging method to extrapolate the scattering amplitude to back-to-back kinematics [36].

Nevertheless, when one compares these calculations in more detail, one finds that the maximum gap and the density dependence vary appreciably among the different approaches (for a review on superfluidity of neutron matter and a compilation of the results, see the recent notes by Lombardo and Schulze [42]). Consequently, further studies are needed in order to improve the microscopic calculations and in order to make reliable predictions of superfluid properties of neutron stars. The RG approach offers a systematic framework for computing the quasiparticle scattering amplitude, which is needed in the calculation of the superfluid gap. In this paper we have presented a straightforward application of the RG method, where both momentum scales, q and q' , are treated on the same footing, and consequently the antisymmetry of the scattering amplitude is preserved. Moreover, the RG method can provide a unifying and transparent framework for the particle-particle and particle-hole effects. Finally, by using the unique low momentum interaction $V_{\text{low } k}$ as the direct interaction, much of the model dependence is removed.

We estimate the 1S_0 pairing gap using weak coupling BCS theory. The pairing

matrix element averaged over the Fermi surface is given by¹³

$$\langle \mathcal{A} \rangle = \frac{1}{8} \int_{-1}^1 d \cos \theta_{\mathbf{q}} \left\{ A(q, \sqrt{4k_F^2 - q^2}) - 3 B(q, \sqrt{4k_F^2 - q^2}) \right\}, \quad (32)$$

where the momenta for back-to-back scattering are constrained by $q^2 + q'^2 = 4k_F^2$. An estimate of the superfluid gap is then given by the weak coupling formula [44]

$$\Delta = 2 \varepsilon_F \exp\left(\frac{1}{\langle \mathcal{A} \rangle}\right), \quad (33)$$

where $\varepsilon_F = k_F^2/2m^*$ denotes the Fermi energy and we use the same prefactor as Ainsworth *et al.* [16,17]. For liquid ^3He , the weak coupling BCS results for the critical temperature are in remarkable agreement with experiment when experimental Fermi liquid parameters are used as input [44,45]. For the direct interaction, the pairing gap, Eq. (33), with a free single particle spectrum is given by

$$\Delta = \frac{k_F^2}{m} \exp\left(\frac{\pi}{2 k_F m V_{\text{low } k}(k_F, k_F; \Lambda = \sqrt{2} k_F; {}^1S_0)}\right). \quad (34)$$

In Fig. 8 we show the superfluid gap computed with the direct term only, Eq. (22), as well as that obtained with the RG solution for the scattering amplitude. To facilitate the comparison with other calculations, the gap obtained with the direct interaction is given for a free single particle spectrum, i.e., $m^*/m = z_{k_F} = 1$. The full solution of the BCS equation using various free nucleon-nucleon interactions yields a maximum gap of about 3 MeV at a Fermi momentum of $0.8 - 0.9 \text{ fm}^{-1}$ (for an overview of the results see Fig. 2 in [42]; see also [46,47,48]). The agreement of the weak coupling result using $V_{\text{low } k}$, Eq. (33), with these calculations is remarkably good. The reason for this success is presumably that in $V_{\text{low } k}$, the strong short-range repulsive core is eliminated, whereas the phase shifts are preserved. For such a “weak” interaction, the weak coupling treatment is expected to work.

In the full RG calculation, including particle-hole polarization effects, we find a much smaller gap; the maximum gap is 0.8 MeV at a Fermi momentum of $k_F = 0.8 \text{ fm}^{-1}$. Here, both the effective mass and the quasiparticle strength $z_{k_F}^2$ are taken into account in the quasiparticle scattering amplitude. The gap is in good agreement with that obtained by Wambach *et al.* [17], which is

¹³ The factor 1/8 in Eq. (32) consists of a factor 1/2 for the average over $\cos \theta_{\mathbf{q}}$, another factor 1/2 for the reduction of the full density of states to that of one spin species. The remaining factor 1/2 accounts for the normalization of the antisymmetrized contact interaction employed in the standard derivation of the weak coupling result (see e.g., [43]).

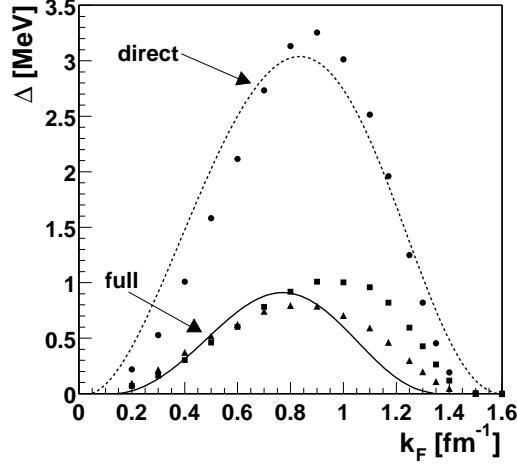


Fig. 8. The 1S_0 superfluid gap versus the Fermi momentum k_F . The dots denote the direct contribution only ($m^*/m = z_{k_F} = 1$), whereas the squares (constant z_{k_F} factor) and the triangles (adaptive z_{k_F} factor) are calculated from the full RG solution. In comparison we show the values of the gap calculated by solving the full BCS equation (dashed line), taken from [42]. The superfluid gap including particle-hole polarization effects obtained by Wambach *et al.* [17] is shown as a solid line.

shown for comparison in Fig. 8. The results obtained in other calculations, which include polarization effects, are compiled in Fig. 7 of [42].

We observe that the full gap vanishes at $k_F = 1.45 \text{ fm}^{-1}$ both for a constant and an adaptive z_{k_F} factor. Moreover, at the lowest Fermi momentum we considered, $k_F = 0.2 \text{ fm}^{-1}$, the ratio of the full to the direct gap is given by $\Delta/\Delta_0 = 0.43$, which is close to the universal low density limit $\Delta/\Delta_0 = (4e)^{-1/3} \approx 0.45$ [49].¹⁴

In the direct interaction, $V_{\text{low } k}$, particle-particle ladder diagrams are included for large relative momenta, $k > \Lambda_{V_{\text{low } k}}$. In fact, we argued that the cutoff accounts for the Pauli blocking of intermediate particle states. This raises the question of double counting, since the BCS equation also sums particle-particle ladders. However, since the gap is generated by low-lying two-particle and two-hole states, which are excluded in $V_{\text{low } k}$ due to the cutoff at $\sqrt{2}k_F$, the double

¹⁴ We note that the low density limit for the ratio of the full to the direct S-wave gap is independent of the scattering length. While the strict low density expansion in $k_F a_S$ is not relevant to neutron star matter, since its validity is restricted to densities below neutron drip, an expansion in an effective scattering length $k_F a_{\text{eff}}$ may be valid up to much higher densities. As argued in [8], $V_{\text{low } k}(0, 0; \Lambda_{V_{\text{low } k}} \sim k_F)$ can be interpreted as the effective scattering length in the particle-particle channel. In the isotriplet channel $V_{\text{low } k}(0, 0) \approx 2.0 \text{ fm}$ in the cutoff independent region. If one adopts the effective scattering length, it is not surprising to find a ratio close to the universal one at $k_F = 0.2 \text{ fm}^{-1}$, since $k_F \ll 1/|a_{\text{eff}}| \approx 0.5 \text{ fm}^{-1}$.

counting problem is minimal. Furthermore, because the cutoff dependence of $V_{\text{low } k}$ is very weak in the density range relevant for superfluidity, any residual double counting, due e.g., to states above the cutoff that contribute to the solution of the BCS gap equation, would not affect our results significantly.

We note that by using a density dependent cutoff, we recover the correct low density limit, where the effective neutron-neutron interaction is given by the free T matrix. This follows because the low momentum interaction $V_{\text{low } k}$ approaches the T matrix for momenta below the inverse S-wave scattering length, i.e., $\Lambda_{V_{\text{low } k}} \sim k_F \ll 1/|a_S|$, as shown in Fig. 5 of [14]. In particular, $V_{\text{low } k}(k_F, k_F) \rightarrow a_S/m$, as $k_F \rightarrow 0$,¹⁵ and we recover the well known low density results in Eq. (34), where the gap is given by the phase shifts [50]. However, due to the large neutron-neutron scattering length, the low density expansion is applicable only for Fermi momenta below $k_F \ll 1/|a_S| = 0.05 \text{ fm}^{-1}$, which corresponds to extremely small densities, well below neutron drip. Since neutron star matter at such densities is in a solid phase, the strict low density expansion in $k_F a_S$ is not relevant for the physics of neutron stars.

Finally, we remark that the physical pairing gap is given by $z_{k_F} \Delta$. Thus, our results should be multiplied by the quasiparticle strength given in Fig. 5.¹⁶ We stress that the physical effect responsible for the strong reduction of the gap is the polarization by the many-body medium. A detailed analysis of the influence of self-energy contributions on the superfluid gap can be found in [33,51,52].

Particle-hole polarization may have a strong effect also on the color superconducting gap in high density QCD. We plan to explore these effects using the methods presented here in future studies.

4.3 The equation of state of neutron matter

In contrast to nuclear matter, neutron matter does not saturate. It is stable only if the positive pressure is balanced by an external force, as e.g., gravitation in a neutron star. Therefore, it is possible to compute the equation of state of neutron matter using the Fermi liquid parameters presented in Section 4.1. This method, which accounts for polarization effects on the equation of state, was first employed by Källman [15].

The speed of sound c_s of a Fermi liquid is given by the incompressibility K [53]

¹⁵ In [14] conventional units are used where $\hbar^2/m = 1$.

¹⁶ Given the uncertainty in the pre-exponential factor of Eq. (33), this may seem superfluous. However, for a given prefactor, it leads to an additional suppression of the gap.

$$c_S^2 = \frac{dP}{d\rho} = \frac{1}{9m} K, \quad (35)$$

where ρ denotes the mass density and K is the incompressibility. The latter is in Fermi liquid theory given by

$$K = \frac{3 k_F^2 (1 + F_0)}{m (1 + F_1/3)}. \quad (36)$$

In the density range of interest, the neutrons may to a good approximation be treated non-relativistically. Thus, the mass density is given by $\rho = m n$, where $n = k_F^3/3\pi^2$ is the number density. Now, we can solve the differential equation

$$\frac{dP}{dn} = \frac{1}{9} K \quad (37)$$

for the equation of state $P(n)$. The incompressibility is computed at each density using the Fermi liquid parameters obtained in the RG approach. The energy per neutron is then computed by integrating the thermodynamic relation

$$P = n^2 \frac{d(E/A)}{dn}. \quad (38)$$

This approach requires two initial conditions for the differential equations, Eqs. (37,38). One can match our results with a conventional equation of state $P_C(n)$ at a certain matching density n_M . For $n > n_M$, the resulting equation of state $\tilde{P}(n)$ reads

$$\tilde{P}(n) = P(n) - P(n_M) + P_C(n_M), \quad (39)$$

with a corresponding equation for the energy per particle. We match the pressure and the energy to the $V_{\text{low k}}$ Hartree-Fock equation of state at the density $n = 0.02 \text{ fm}^{-3}$. This is the lowest density given by Akmal *et al.* [54].¹⁷ We stress that the equation of state depends on the matching condition. The energy is particularly sensitive, since it requires two constants of integration. Below we give a parametrization of the pressure, with the boundary condition $P(n=0) = 0$,

$$P(n) = 79.09 \left(\frac{n}{\text{fm}^{-3}} \right)^{5/3} \left\{ 1.000 - 1.177 \left(\frac{n}{\text{fm}^{-3}} \right)^{1/3} - 0.324 \left(\frac{n}{\text{fm}^{-3}} \right) + 5.290 \left(\frac{n}{\text{fm}^{-3}} \right)^2 \right\} \frac{\text{MeV}}{\text{fm}^3}. \quad (40)$$

With this parametrization, the reader can match our equation of state to a conventional one at low densities.

¹⁷ At very low densities the Hartree-Fock calculation cannot be trusted due to the large neutron-neutron scattering length, as discussed above.

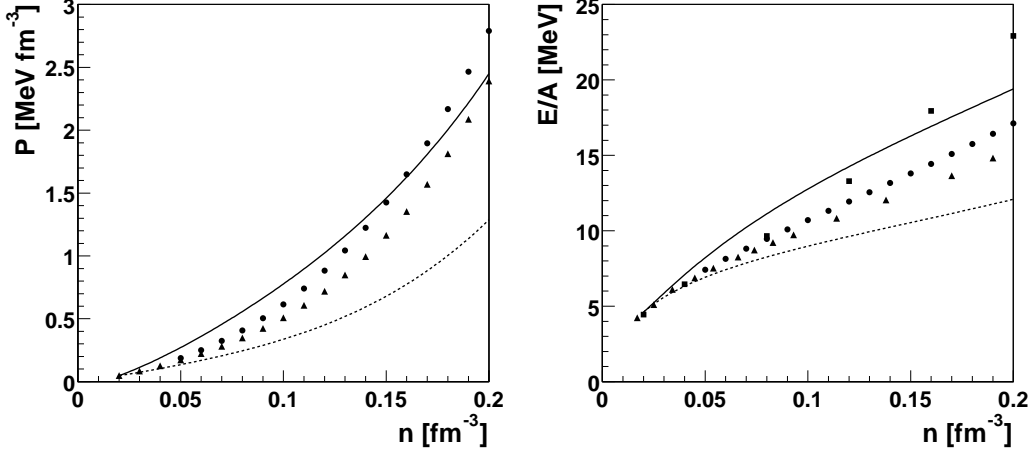


Fig. 9. The pressure P and the energy per neutron E/A for pure neutron matter as functions of density n . Results are given for the full Fermi liquid parameters (solid line) and the direct ones (dashed line) matched to the $V_{\text{low } k}$ Hartree-Fock equation of state at low density, $n = 0.02 \text{ fm}^{-3}$. Also given is the $V_{\text{low } k}$ Hartree-Fock contribution to the energy [55] and the pressure calculated by means of Eq. (38) (triangles). In comparison, we show the Brueckner-Hartree-Fock equation of state of Bao *et al.* [56] (dots) computed with the non-relativistic Bonn potential and the equation of state of Akmal *et al.* [54] (squares) from a variational calculation using the Argonne v_{18} interaction supplemented by three-body forces and the boost corrections. For a comparison with other equations of state, see also Fig. 1 in Lattimer and Prakash [57].

The resulting pressure and the energy per neutron are shown in Fig. 9. We note that the Hartree-Fock energy obtained with $V_{\text{low } k}$ and the energy obtained from the direct Landau parameters do not coincide. This is solely due to the density dependence of the cutoff $\Lambda_{V_{\text{low } k}}$, which gives rise to additional contributions to the effective interaction. However, since a major part of these contributions correspond to particle-hole propagation in the ZS' channel, they are to a large extent part of the induced interaction and should not be included in the direct term. Consequently, the difference between the Hartree-Fock energy and that obtained using the full induced interaction is due to higher order particle-hole polarization effects [10].

Relative to the $V_{\text{low } k}$ Hartree-Fock calculation [55] there is an increase in pressure and energy below nuclear matter density. Compared to other non-relativistic equations of state [56,54], the pressure and energy is somewhat larger at low densities.¹⁸ At densities above 0.11 fm^{-3} , corresponding to Fermi momenta $k_F > 1.5 \text{ fm}^{-1}$, the resulting z_{k_F} factor is larger than that found in Brueckner-Hartree-Fock calculations, as noted above. A smaller z_{k_F} factor would reduce the attractive contribution from F_0 and thus lead to an increase

¹⁸ The equation of state of Akmal *et al.* is significantly stiffer at higher densities due to three-body forces.

of the incompressibility and consequently also of the pressure and the energy for $n > 0.11 \text{ fm}^{-3}$ in our calculation. We conclude that polarization effects possibly have an important impact on the equation of state, which should be included in a consistent treatment of neutron star superfluidity and neutron star structure.

5 Summary and conclusions

In this work, we have developed a practicable framework for renormalization group calculations of strongly interacting Fermi systems. We employed the RG approach to compute the quasiparticle interaction and the scattering amplitude on the Fermi surface for neutron matter, which for many purposes is a good approximation to neutron star matter, where there is a small admixture of protons. Our approach follows the ideas of Shankar in applying RG techniques to the interacting fermion problem [6,19].

RG methods used to solve multi-channel problems have several advantages. First, all channels and the corresponding momentum scales can be treated on equal footing in a systematic way, which can accommodate fundamental symmetries, such as the Pauli principle. In this study, we considered the RG flow in the particle-hole channels at the one-loop level. An expansion in momentum transfers was performed, which enabled us to compute the beta functions analytically. We note that it is fairly straightforward to include the particle-particle channel in the RG equations for the scattering amplitude and the quasiparticle interaction. This opens the possibility to explore the interference of the particle-hole and particle-particle channels. A calculation of this kind corresponds to solving the “parquet equations at the one-loop order”. The expansion in momentum transfers can be removed by computing the complete particle-hole phase space [12].

In contrast to the traditional approach to the many-body problem, the RG adapts the starting vacuum interaction to include the in medium effects due to the fastest particle-hole excitations. In the subsequent iteration, this renormalized interaction is modified to account for the next fastest modes. Therefore, at every step, the flow of the effective interaction is expanded around the current system, which highlights the efficacy of the approach. Moreover, the RG flow is physically very transparent, since the effects of the high momentum modes are readily tractable. We believe that the RG method is a promising tool for studying a wide range of nuclear many-body problems.

At the one-loop level and at zero temperature the RG equations are particularly transparent. We found an ambiguous long-wavelength limit, analogous to that appearing in the original treatment of Landau, which can be used to

distinguish between the quasiparticle interaction and the forward scattering amplitude. This implies that, at the one-loop level, it is necessary to solve only the RG equation for the scattering amplitude. The quasiparticle interaction is then obtained in the corresponding limit. A test for the consistency of the solution is provided by general relations between the forward scattering amplitude and the Fermi liquid parameters.

We solved the RG equations in the particle-hole channels for neutron matter, where tensor interactions are absent in relative S-states. The RG flow includes the exchange channel, and thus it builds up the polarization effects of the induced interaction of Babu and Brown. Our results for neutron matter are very encouraging and provide strong motivation for further developments of the RG approach to the nuclear many-body problem as well as for condensed matter systems.

In the calculation, polarization and self-energy effects have been treated self-consistently. The latter have been included in a simple approximation, which nevertheless led to good quantitative results at intermediate densities.

Results for the Fermi liquid parameters and the scattering amplitude for the density range of interest to neutron stars were presented. The Fermi liquid parameters satisfy the Pauli principle sum rules by construction. Moreover, polarization effects lead to an enhancement in the pressure and the energy per neutron below nuclear matter density. As a first application, which probes the momentum dependence of the scattering amplitude, we computed the 1S_0 superfluid gap using weak coupling BCS theory. A reduction from a direct gap of 3.3 MeV to 0.8 MeV was found. Our results confirm the importance of particle-hole polarization effects for superfluidity. A further application of the scattering amplitude at finite momentum transfers is in calculations of transport processes.

For a similar analysis of nuclear matter, it is necessary to extend the flow equations to incorporate tensor interactions. These are important for a complete discussion of nuclear matter, and we expect rather large renormalization effects from the arguments given in [8]. Moreover, tensor correlations and the tensor Fermi liquid parameters play an important role in the physics of dense matter [58]. As noted in the introduction, tensor forces are less pronounced in neutron matter, since they are not operative in relative S-states. However, for specific quantities the tensor force may be of crucial importance.

To date, polarization effects on the 3P_2 – 3F_2 pairing of neutrons have not been addressed and a quantitative analysis is very much needed. Pethick and Ravenhall argue that both density and spin-density fluctuations would increase the gap in this state and thus possibly extend the superfluid regime to lower densities [39]. Once the RG approach is adapted to allow for tensor forces, it should

be straightforward to address this problem [59].

Acknowledgements

We thank Tom Kuo and Scott Bogner for providing us with the $V_{\text{low } k}$ code and Kevin Bedell, Vincent Brindejonc and Janos Polonyi for rewarding discussions. AS thanks the Theory Group at GSI for their kind hospitality. The work of AS and GEB is supported by the US-DOE grant No. DE-FG02-88ER40388.

A Derivation of the Fermi liquid theory results from the ZS channel beta function

For a one channel problem, such as the interacting Fermi system restricted to the ZS channel, the one-loop RG is equivalent to solving the Bethe-Salpeter equation in that channel. We define the fast particle-hole Lindhard function at $\omega = 0$ by integrating out the fast modes

$$\chi(q, \Lambda) = g \int_{\text{fast}, \Lambda} \frac{d^3 \mathbf{p}''}{(2\pi)^3} \frac{n_{\mathbf{p}''+\mathbf{q}/2} - n_{\mathbf{p}''-\mathbf{q}/2}}{\varepsilon_{\mathbf{p}''+\mathbf{q}/2} - \varepsilon_{\mathbf{p}''-\mathbf{q}/2}}. \quad (\text{A.1})$$

For $q \ll k_F$, we expand and write the particle-hole phase space explicitly at zero temperature

$$\begin{aligned} \chi(q, \Lambda) = g \int \frac{d^3 \mathbf{p}''}{(2\pi)^3} \frac{1}{v_F q \cos \theta} \\ \times \left[\Theta(k_F - \Lambda - (p'' + q \cos \theta/2)) \Theta((p'' - q \cos \theta/2) - (k_F + \Lambda)) \right. \\ \left. - \Theta((p'' + q \cos \theta/2) - (k_F + \Lambda)) \Theta(k_F - \Lambda - (p'' - q \cos \theta/2)) \right], \end{aligned} \quad (\text{A.2})$$

where the occupation numbers are automatically taken care of by the Θ functions that define the border between the fast and slow modes and θ denotes the angle between \mathbf{p}'' and \mathbf{q} . We rewrite the product of theta functions using

$\Theta(\Lambda_1 - x) \Theta(x - \Lambda_2) = (\Theta(x - \Lambda_2) - \Theta(x - \Lambda_1)) \Theta(\Lambda_1 - \Lambda_2)$. This leads to

$$\begin{aligned} \chi(q, \Lambda) &= g \int \frac{d^3 \mathbf{p}''}{(2\pi)^3} \frac{1}{v_F q \cos \theta} \\ &\times \left[\left\{ \Theta(p'' - q \cos \theta/2 - k_F - \Lambda) - \Theta(p'' + q \cos \theta/2 - k_F + \Lambda) \right\} \right. \\ &\times \Theta(-q \cos \theta - 2\Lambda) - \left\{ \Theta(p'' + q \cos \theta/2 - (k_F + \Lambda)) \right. \\ &\left. \left. - \Theta(p'' - q \cos \theta/2 - k_F + \Lambda) \right\} \Theta(q \cos \theta - 2\Lambda) \right]. \end{aligned} \quad (\text{A.3})$$

When we differentiate with respect to the cutoff, the contributions from the multiplicative theta functions $\Theta(\pm q \cos \theta - 2\Lambda)$ vanish, since for $q \cos \theta/2 = \pm \Lambda$ the two remaining theta functions cancel. Moreover, $q \ll k_F$ implies $\Lambda \ll k_F$, which leads to

$$\begin{aligned} \frac{d\chi(q, \Lambda)}{d\Lambda} &= g \int \frac{d^3 \mathbf{p}''}{(2\pi)^3} \frac{1}{v_F q \cos \theta} 2 \delta(p'' - k_F) \left[\Theta(q \cos \theta - 2\Lambda) \right. \\ &\left. - \Theta(-2\Lambda - q \cos \theta) \right] \end{aligned} \quad (\text{A.4})$$

$$= \frac{2}{q} \frac{g m^* k_F}{2 \pi^2} \int_{2\Lambda/q < |\cos \theta| < 1} \frac{d\Omega_{\mathbf{p}''}}{4\pi} \frac{\text{sign}(\cos \theta)}{\cos \theta} \Theta(q - 2\Lambda). \quad (\text{A.5})$$

This leads to the RG equation, Eq. (7). Under restriction to the ZS channel, we find after projecting the scattering amplitude on Legendre polynomials

$$a = \sum_l a_l(\Lambda) P_l(\cos \theta_{q'}) \quad (\text{A.6})$$

$$\frac{da_l(\Lambda)}{d\Lambda} = -\frac{g m^* k_F}{2 \pi^2} \frac{2}{q} \log\left(\frac{2\Lambda}{q}\right) \frac{a_l(\Lambda)^2}{2l+1} \Theta(q - 2\Lambda), \quad (\text{A.7})$$

where we have set $z_{k_F} = 1$ for simplicity. We propose to think of q as an external scale, since it must be kept finite and may only be set to zero after integrating the RG equation. The solution of the RG equation in one channel, Eq. (A.7), is obtained by integrating from the initial condition $a_l(\Lambda = q/2) = a_l^{(0)}$ to $\Lambda = 0$. We find

$$a_l = \frac{a_l^{(0)}}{1 + \frac{g m^* k_F}{2 \pi^2} \frac{a_l^{(0)}}{2l+1}}, \quad (\text{A.8})$$

which are the standard Fermi liquid theory relations among the quasiparticle interaction and the forward scattering amplitude after identifying $A_l = \frac{g m^* k_F}{2 \pi^2} a_l$ and $F_l = \frac{g m^* k_F}{2 \pi^2} a_l^{(0)}$. The RG initial condition being the Fermi liquid parameters is understood, since we assume that the flow in the ZS' channel

has been carried out to build up the quasiparticle interaction or equivalently the Fermi liquid parameters are taken from experimental measurements.

References

- [1] L.D. Landau, Sov. Phys. JETP **3** (1957) 920.
- [2] L.D. Landau, Sov. Phys. JETP **5** (1957) 101.
- [3] L.D. Landau, Sov. Phys. JETP **8** (1959) 70.
- [4] G. Baym and C.J. Pethick, Landau Fermi Liquid Theory: Concepts and Applications, Wiley, New York, 1991.
- [5] S. Babu and G.E. Brown, Ann. Phys. **78** (1973) 1.
- [6] R. Shankar, Rev. Mod. Phys. **66** (1994) 129.
- [7] J. Polchinski, in Proceedings of the 1992 Theoretical Advanced Studies Institute in Elementary Particle Physics, Eds. J. Harvey and J. Polchinski, World Scientific, Singapore, 1993, hep-th/9210046.
- [8] A. Schwenk, G.E. Brown and B. Friman, Nucl. Phys. **A703** (2002) 745.
- [9] K.S. Bedell and T.L. Ainsworth, Phys. Lett. **102A** (1984) 49.
- [10] O. Sjöberg, Ann. Phys. **78** (1973) 39.
- [11] S.-O. Bäckman, G.E. Brown and J.A. Niskanen, Phys. Rept. **124** (1985) 1.
- [12] V. Brindejone and B. Friman, in preparation.
- [13] S.K. Bogner, T.T.S. Kuo and L. Coraggio, Nucl. Phys. **A684** (2001) 432c.
- [14] S.K. Bogner, T.T.S. Kuo, A. Schwenk, D.R. Entem and R. Machleidt, nucl-th/0108041.
- [15] C.-G. Källman, Nucl. Phys. **A213** (1973) 461.
- [16] T.L. Ainsworth, J. Wambach and D. Pines, Phys. Lett. **B222** (1989) 173.
- [17] J. Wambach, T.L. Ainsworth and D. Pines, Nucl. Phys. **A555** (1993) 128.
- [18] K.G. Wilson and J.B. Kogut, Phys. Rept. **12** (1974) 75.
- [19] R. Shankar, Physica **A177** (1991) 530.
- [20] N. Dupuis, Eur. Phys. J. **B3** (1998) 315.
- [21] G. Benfatto and G. Gallavotti, Phys. Rev. **B42** (1990) 9967.
- [22] G. Benfatto and G. Gallavotti, J. Stat. Phys. **59** (1990) 541.

- [23] J. Feldman, D. Lehmann, H. Knörrer and E. Trubowitz, in *Constructive Physics*, Springer Lectures Notes in Physics, Ed. V. Rivasseau, Vol. 446 (1995) 267.
- [24] N. Dupuis and G.Y. Chitov, *Phys. Rev.* **B54** (1996) 3040.
- [25] A.C. Hewson, *Adv. Phys.* **43** (1994) 543.
- [26] S.-O. Bäckman, O. Sjöberg and A.D. Jackson, *Nucl. Phys.* **A321** (1979) 10.
- [27] S.-O. Bäckman, C.-G. Källman and O. Sjöberg, *Phys. Lett.* **B43** (1973) 263.
- [28] T.L. Ainsworth, K.S. Bedell, G.E. Brown and K.F. Quader, *J. Low Temp. Phys.* **50** (1983) 317.
- [29] T.L. Ainsworth and K.S. Bedell, *Phys. Rev.* **B35** (1987) 8425.
- [30] B.L. Friman and A.K. Dhar, *Phys. Lett.* **B85** (1979) 1.
- [31] J.P. Jeukenne, A. Lejeune and C. Mahaux, *Phys. Rept.* **25** (1976) 83.
- [32] W. Zuo, G. Giansiracusa, U. Lombardo, N. Sandulescu and H.-J. Schulze, *Phys. Lett.* **B421** (1998) 1.
- [33] M. Baldo and A. Grasso, *Phys. Lett.* **B485** (2000) 115.
- [34] A. Schwenk, B. Friman, S.K. Bogner, G.E. Brown and T.T.S. Kuo, Talk given at 5th Int. Conference Renormalization Group 2002, Tatranská Štrba, Slovakia, March, 2002, *Acta Phys. Slov.* **52** (2002) 207.
- [35] A.D. Jackson, E. Krotschek, D.E. Meltzer and R.A. Smith, *Nucl. Phys.* **A386** (1982) 125.
- [36] H.-J. Schulze, J. Cugnon, A. Lejeune, M. Baldo and U. Lombardo, *Phys. Lett.* **B375** (1996) 1.
- [37] K. Bedell, private communication.
- [38] J.W. Clark, C.-G. Källman, C.-H. Yang and D.A. Chakalakal, *Phys. Lett.* **B61** (1976) 331.
- [39] C.J. Pethick and D.G. Ravenhall, *Ann. N.Y. Acad. Sci.* **647** (1991) 503.
- [40] J.M.C. Chen, J.W. Clark, E. Krotschek and R.A. Smith, *Nucl. Phys.* **A451** (1986) 509.
- [41] J.M.C. Chen, J.W. Clark, R.D. Davé and V.V. Khodel, *Nucl. Phys.* **A555** (1993) 59.
- [42] U. Lombardo and H.-J. Schulze, in *Physics of Neutron Star Interiors*, Springer Lecture Notes in Physics, Eds. D. Blaschke, N.K. Glendenning and A. Sedrakian, Vol. 578 (2001) 30, astro-ph/0012209.
- [43] A.A. Abrikosov, L.P. Gor'kov and I.E. Dzyaloshinski, *Methods of Quantum Field Theory in Statistical Physics*, Dover, New York, 1963.

- [44] B.R. Patton and A. Zaringhaleh, Phys. Lett. **A55** (1975) 95.
- [45] K. Bedell and D. Pines, Phys. Lett. **A95** (1980) 281.
- [46] M. Baldo, J. Cugnon, A. Lejeune and U. Lombardo, Nucl. Phys. **A515** (1990) 409.
- [47] V.A. Khodel, V.V. Khodel and J.W. Clark, Nucl. Phys. **A598** (1996) 390.
- [48] Ø. Elgarøy and M. Hjorth-Jensen, Phys. Rev. **C57** (1998) 1174.
- [49] L.P. Gorkov and T.K. Melik-Barkhudarov, Sov. Phys. JETP **13** (1961) 1018.
- [50] V.J. Emery and A.M. Sessler, Phys. Rev. **119** (1960) 248.
- [51] P. Bozek, Nucl. Phys. **A657** (1999) 187.
- [52] U. Lombardo, P. Schuck and W. Zuo, Phys. Rev. **C64** (2001) 021301(R).
- [53] P. Nozières, Theory of Interacting Fermi Systems, Addison-Wesley, Reading, Massachusetts, 1997.
- [54] A. Akmal, V.R. Pandharipande and D.G. Ravenhall, Phys. Rev. **C58** (1998) 1804.
- [55] A. Schwenk, Ph.D. Thesis, SUNY Stony Brook, 2002.
- [56] G. Bao, L. Engvik, M. Hjorth-Jensen, E. Osnes and E. Østgaard, Nucl. Phys. **A575** (1994) 707.
- [57] J.M. Lattimer and M. Prakash, Astrophys. J. **550** (2001) 426.
- [58] E. Olsson and C.J. Pethick, Talk given at Compact Stars in the QCD Phase Diagram, Copenhagen, 2001, astro-ph/0203011.
- [59] A. Schwenk, B. Friman and G.E. Brown, in preparation.